

A Petrophysical Assessment of the Ireton Caprock Sealing Capacity by Integrating Lithofacies and Mercury Injection Capillary Pressure Analyses

Huiju Geng, Tyler Hauck, Baohong Yang, David Herbers
Alberta Energy Regulator (AER) - Alberta Geological Survey (AGS)

Summary

Carbon Capture, Utilization, and Storage (CCUS) as a strategy for decarbonizing Canada's petroleum industry is receiving significant attention prompting the Alberta Geological Survey to study opportunities for CCUS in central Alberta. The Upper Devonian Leduc Formation, comprising variably dolomitized reef systems that have been prolific conventional oil and gas reservoirs since the late 1940s, is currently a prospective target for CCUS now that many of the conventional reservoirs are depleted. The overlying Upper Devonian Ireton Formation has served as a regional caprock to the Leduc reservoirs. With the prospect of CCUS within the Leduc, the Ireton Formation requires study to evaluate the sealing capacity and integrity of the caprock to keep the injected CO₂ in place. This study focuses on evaluating the caprock seal capacity and identifying areas where the sealing capacity may be compromised. The study employs a multifaceted approach with a detailed analysis of lithofacies, Mercury Injection Capillary Pressure (MICP) tests, petrophysical interpretations, and Monte-Carlo simulations. Results include a comprehensive regional distribution of the Ireton sealing capacity. Whereas most areas demonstrate desirable sealing capacity, the area overlying the Bashaw reef trend shows lower entry pressure and threshold pressure suggesting potential weaker seal capacity, which has been shown in previous studies (Hearn et al. 2011). This study also provides a workflow for assessing caprock seal capacity of similar CCUS projects.

Method and Workflow

To better understand the caprock, 12 Ireton Formation cores across the study area were analyzed, and 7 lithofacies were identified (Fig.1). Lithofacies range from non-calcareous argillaceous shale to floatstones with variable argillaceous content. Facies are often interbedded or homogenized through intense bioturbation (Fig. 2). Dolomitic limestone or dolostone was observed rarely within the cores but was found more commonly within carbonate-rich Ireton facies in areas over the Bashaw Complex where the Ireton is thin. Twenty Mercury Injection Capillary Pressure (MICP) tests were performed on samples taken from each facies.

The MICP data were utilized to determine the caprock seal capacity, that is, the column height of CO₂ that the caprock can retain before capillary forces allow the migration of the CO₂ into, and possibly through, the pore system of the caprock (Dewhurst et al., 2002; Kaldi et al., 2011; Celeste et al., 2018; Dewhurst et al., 2019).

At the reservoir-caprock interface, the CO₂ is trapped below the seal until the capillary entry pressure is exceeded. When a trap is filled to its seal capacity, the capillary pressure of the seal is balanced by the upward buoyancy of the CO₂, leading to:

$$P_c = (\rho_b - \rho_{CO_2})gH \quad (1)$$

where P_c is capillary pressure in psi, ρ_b and ρ_{CO_2} are the densities (g/cm³) of brine and CO₂ respectively (assuming the caprock is water-wet), H is the height of the CO₂ column above the free water level, and g is acceleration due to gravity, a constant of 0.433. The height of the CO₂ column corresponding to a specific capillary pressure is calculated as:

$$H = \frac{P_c}{(\rho_b - \rho_{CO_2})g} \quad (2)$$

As capillary pressure data were initially obtained from an air-mercury system, the data must be converted to a brine-CO₂ system prior to performing calculations. Figure 3a illustrates the capillary pressure versus the percentage of total intrusion pore volume of the 20 samples in a brine-CO₂ system, and Figure 3b is derived from Figure 3a through the conversion of pressure to the height of the CO₂ column using equation (2).

A petrophysical assessment was conducted to integrate capillary pressure and lithofacies, extending the interpretation to a regional scale. By calibrating logs with MICP samples, a variety of rock properties were delivered, including mineral abundance, porosity, permeability, and capillary entry pressures.

In addition to the entry pressure, another critical parameter derived from the capillary pressure plot is the threshold pressure. This is considered to be the pressure level at which a continuous filament of non-wetting phase first extends through the pore network of the seal, potentially resulting in the migration of CO₂ through the caprock (Schowalter, 1979; Kivior et al., 2002; Kaldi et al., 2011; Dewhurst et al., 2002, 2019). Figure 4 shows the scatter plot and box chart depicting the MICP threshold pressures of the seven lithofacies. A notable observation from Figure 4 is the general trend of decreasing MICP threshold pressure with an increase in facies number (corresponding to a general increase in carbonate content). Within a regional context, facies 2, 3, and 4 are the most common, while other facies are minor. Considering this, for efficient utilization of the facies data, we consolidated the seven lithofacies into three petrofacies, each with its distinct threshold pressure distribution (Table 1). Subsequently, a supervised machine learning model was developed to predict petrofacies from well logs. Figure 5 presents an instance of log-predicted petrofacies compared to lithofacies interpreted from core. Once petrofacies were determined, a Monte Carlo simulation was executed at each logging depth to simulate the threshold pressure based on log-predicted petrofacies type. At each well location, the P10, P50, and P90 threshold pressure values are provided.

Results and Discussion

The study reveals important insights into the caprock sealing capacity of the Upper Devonian Ireton Formation. Notably, the variability in carbonate content within the Ireton significantly influences sealing potential (see also Hearn et al., 2011). The height of CO₂ column corresponding to the entry pressure and threshold pressure of the 20 MICP samples are summarized in Table 2. Whereas most of the samples require significant entry pressures for CO₂ to move into the rock (114–225 psi), three samples require much lower entry pressures (16.3 – 53.3 psi). While some samples can retain a CO₂ column greater than 100 m before any CO₂ intrusion, the three weak samples can only retain a shorter CO₂ column (27.9–91.5 m). These samples are taken from relatively thin Ireton intervals overlying the Bashaw reef complex with a higher proportion of carbonate material.

Figure 6 illustrates mineralogy distribution within the study area predicted from logs, and Figure 7 presents the distribution of capillary threshold pressure from Monte-Carlo simulation results. A notable observation is the increase in clay abundance and decrease in carbonate content towards the reef margins. Conversely, moving towards the inner lagoonal regions of the reefs, carbonate content increases at the expense of clay. This correlates to the increasing threshold pressure as one passes from the lagoonal to reef margin areas (Fig. 7).

Furthermore, the Monte Carlo simulation results also reveal that the Ireton facies over the Bashaw reef complex have the lowest threshold pressures, which correlates with the measured MICP samples and correlates with both measured and predicted carbonate content.

Acknowledgements

We express our gratitude to session chairs Eva Drivet and David Hills for their assistance with the abstract. We also extend our thanks to Alex MacNeil for his contributions and feedback throughout this study.

References

- Celeste D. Lohr, Paul C. Hackley, 2018. Using mercury injection pressure analyses to estimate sealing capacity of the Tuscaloosa marine shale in Mississippi, USA: Implications for carbon dioxide sequestration. *International Journal of Greenhouse Gas Control* V. 78, p. 375-387
- Dewhurst D.N., Piane C.D., Esteban L., Sarout J., Josh M., Pervukhina M., Clennell M.B., 2019. Microstructural, Geomechanical, and Petrophysical Characterization of Shale Caprocks. In: *Geological Carbon Storage: Subsurface Seals and Caprock Integrity*, Geophysical Monograph 238, First Edition, Edited by Vialle S., Ajo-Franklin J., and Carey J. W.
- Dewhurst D., Jones R., Raven M. 2002. Microstructural and petrophysical characterization of Muderong Shale: application to top seal risking. *Petroleum Geoscience*, v. 8, p. 371–383
- IEA Greenhouse Gas R&D Programme (IEAGHG) (2011/01, June 2011) Caprock systems for CO₂ geological storage.
- Hearn, M.R., Machel, H.G. and Rostron, B.J. 2011. Hydrocarbon breaching of a regional aquitard: the Devonian Ireton Formation, Bashaw area, Alberta, Canada. *American Association of Petroleum Geologists Bulletin*, v. 95, p. 1009–1037.
- Hearn, M. R., 1996, Stratigraphic and diagenetic controls on aquitard integrity and hydrocarbon entrapment, Bashaw Reef Complex, Alberta, Canada: Master's thesis, University of Alberta, Alberta, 135 p.
- Kivior T., Kaldi J.G., Lang S.G. 2002. Seal potential in Cretaceous and late Jurassic rocks of the Vulcan sub-basin, Northwest shelf Australia, *The APPEA Journal*, v. 42, p. 203–224.
- Schwabert, T.T. 1979. Mechanisms of secondary hydrocarbon migration and entrapment. *American Association of Petroleum Geologists Bulletin*, v. 63, p. 723–760.
- Stoakes, F. A., 1980, Nature and growth of shale basin fill and its effect on reef growth and termination: Upper Devonian Duvernay and Ireton formations of Alberta, Canada: *Bulletin of Canadian Petroleum Geology*, v. 28, p. 345–410.

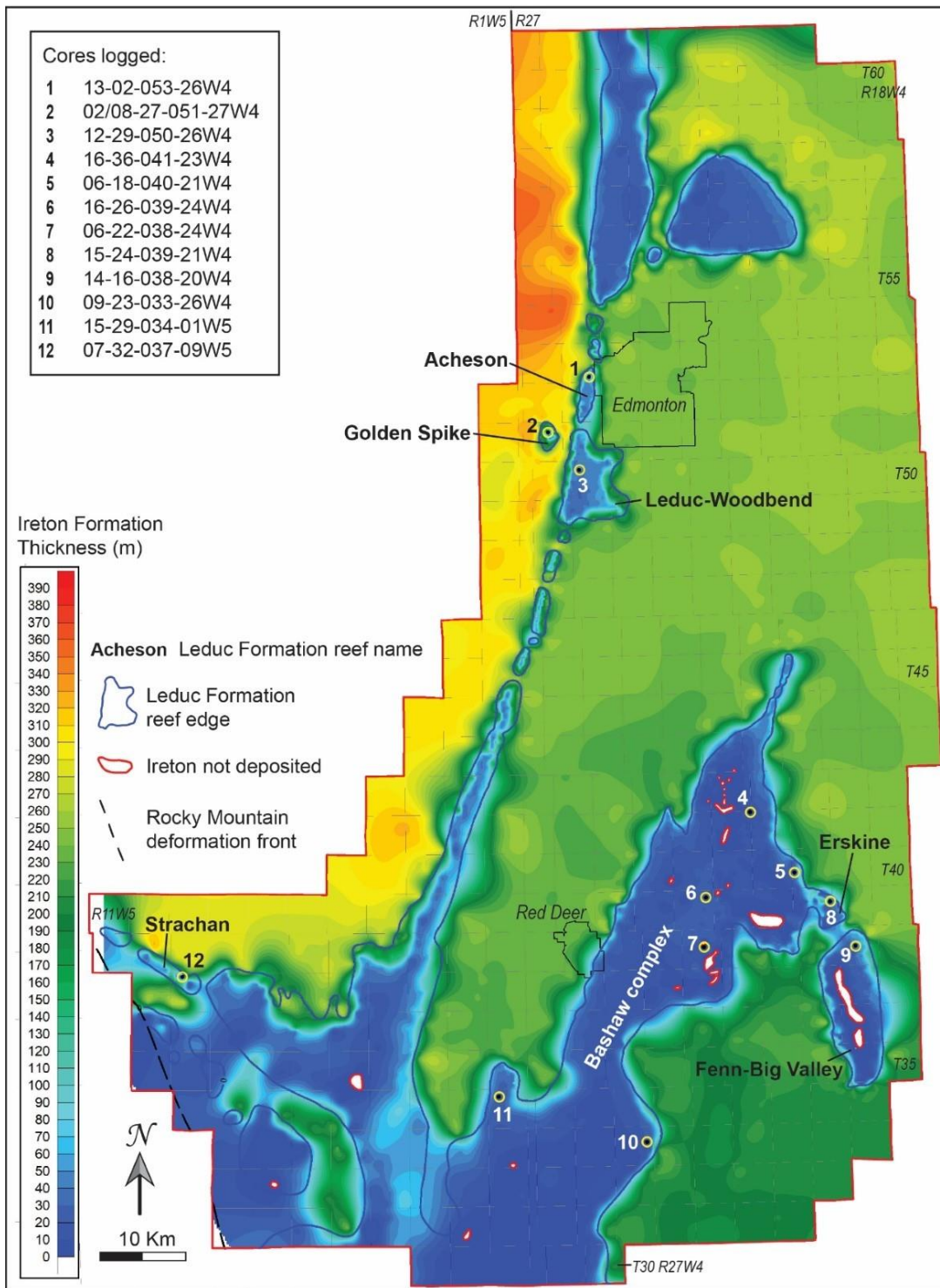


Figure 1. Isopach map of the Ireton Formation within the study area with Leduc Formation reef buildups and location of cores logged for lithofacies and MICP analysis.

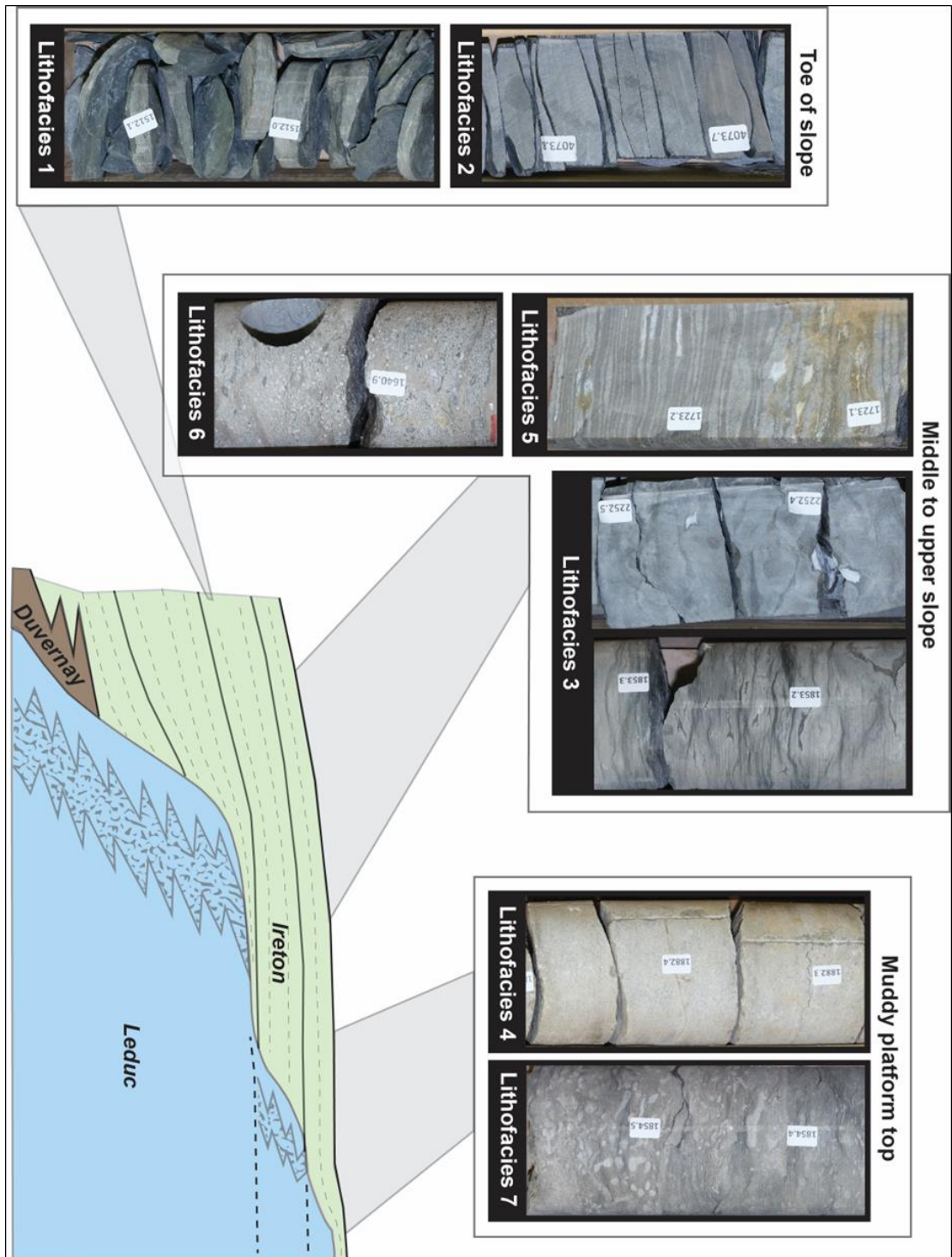


Figure 2. Ireton facies association model, adapted from Stoakes (1980) and Hearn et al. (2011).

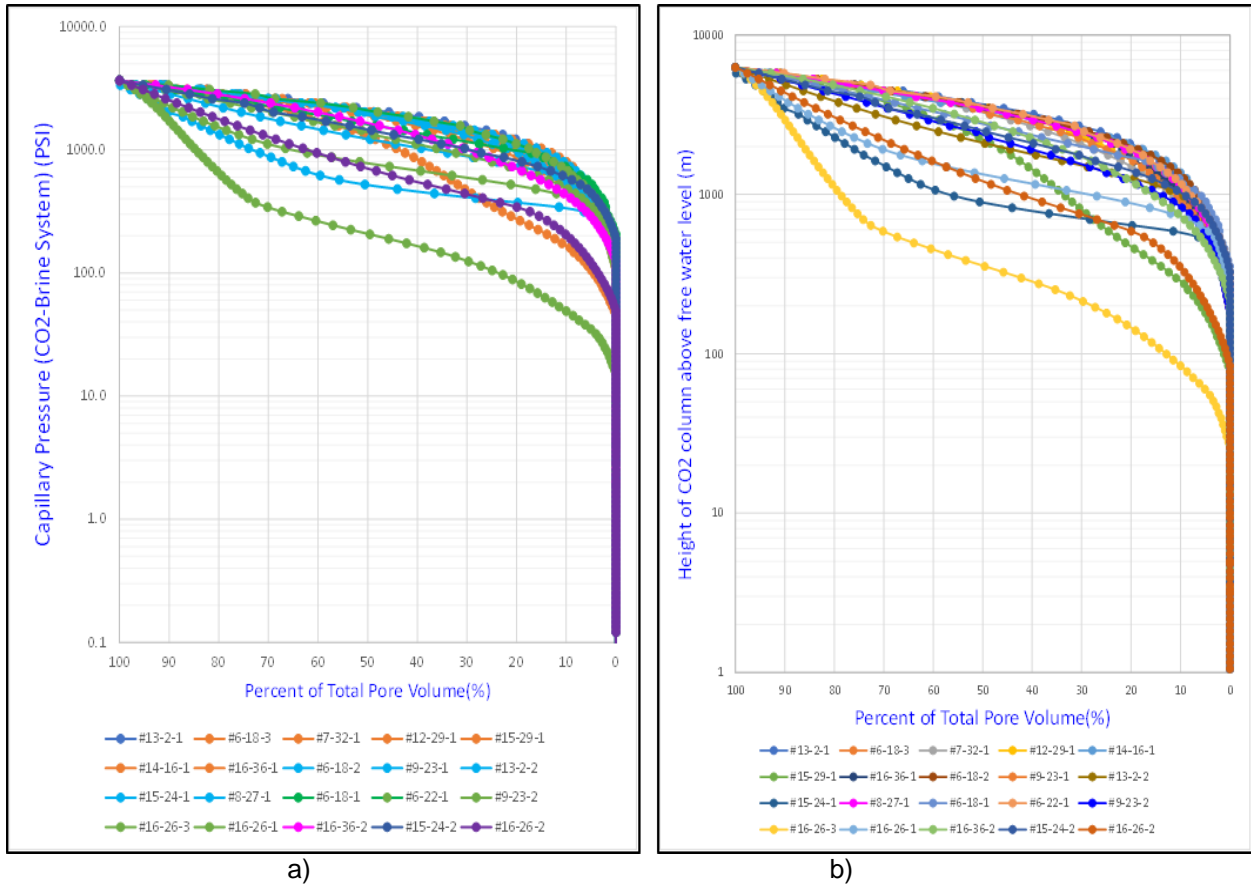


Figure 3. a) Capillary pressure *versus* percent of total intrusion pore volume in brine-CO₂ system. **b)** Height of carbon dioxide column *versus* percent of total intrusion pore volume in brine-CO₂ system.

Table 1. Summary of threshold pressure distribution of 3 consolidated petrofacies.

Facies	Statistical Distribution Parameters				
	Minimum(psi)	Maximum(psi)	Mean(psi)	Standard Deviation(psi)	Count
Petrofacies A	160.1	1118.7	728.0	295.8	7
Petrofacies B	342.5	797.7	564.8	180.8	5
Petrofacies C	32.1	944.6	423.6	268.8	8

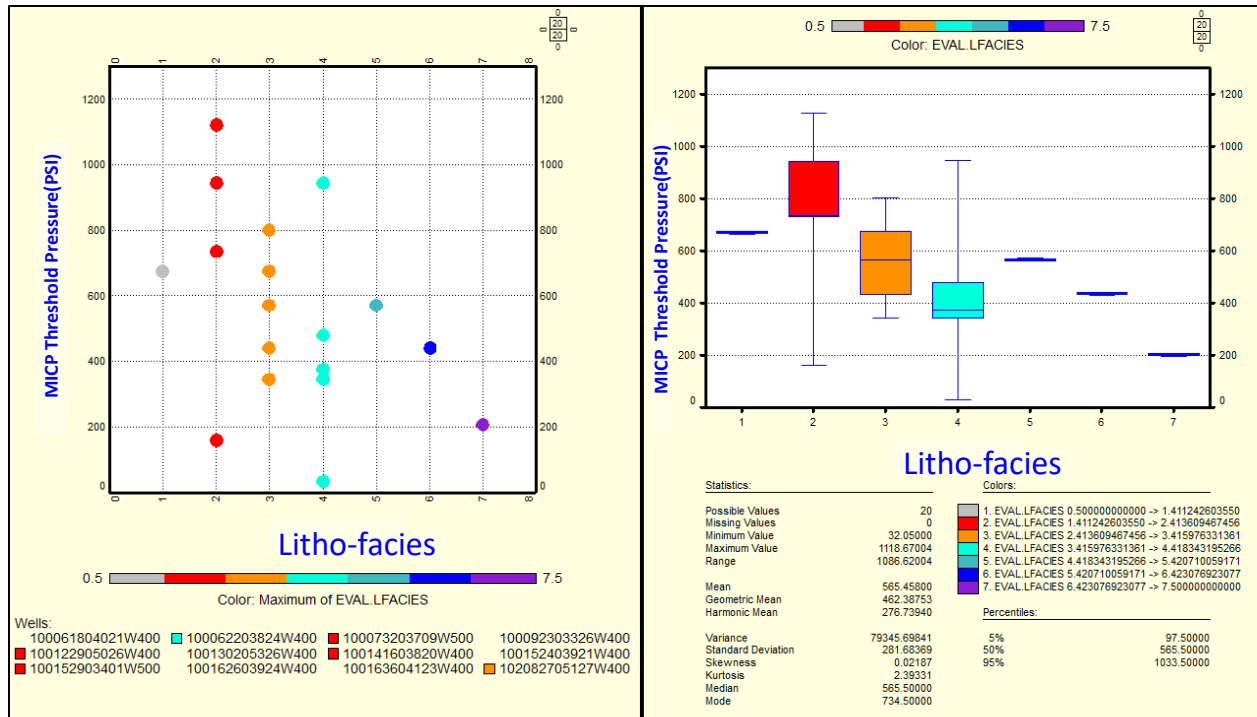


Figure 4. Scatter plot and box plot of threshold pressures of 20 MICP samples from 7 lithofacies.

Table 2. Summary of capillary pressure and calculated heights of CO₂ column of 20 MICP samples.

UWI	Sample_ID	Depth	Porosity	Permeability	Entry Pressure	Threshold Pressure	CO ₂ Column Heights Calculated from Entry Pressure	CO ₂ Column Heights Calculated from Threshold Pressure
		metres	%	md	psi	psi	m	m
100061804021W400	6-18-1	1665.80	1.08	2.04E-05	224.56	480.36	385.6	824.7
100061804021W400	6-18-2	1659.50	1.46	6.93E-05	174.39	797.69	299.4	1369.5
100061804021W400	6-18-3	1650.05	2.21	2.09E-04	114.41	1118.67	196.4	1920.6
100062203824W400	6-22-1	1881.20	1.56	7.66E-05	206.29	944.60	354.2	1621.8
100073203709W500	7-32-1	4060.60	0.90	5.02E-05	174.40	733.13	299.4	1258.7
100092303326W400	9-23-1	2251.40	1.19	9.86E-05	174.39	673.62	299.4	1156.5
100092303326W400	9-23-2	2249.35	2.11	1.22E-04	114.21	372.74	196.1	639.9
100122905026W400	12-29-1	1614.70	1.84	8.81E-05	160.18	733.08	275.0	1258.6
100130205326W400	13-2-1	1515.80	2.39	1.29E-04	174.30	673.59	299.3	1156.5
100130205326W400	13-2-2	1511.60	3.19	3.48E-05	160.02	441.37	274.7	757.8
100141603820W400	14-16-1	1615.00	2.93	1.11E-04	135.18	944.61	232.1	1621.8
100152403921W400	15-24-1	1641.15	3.74	1.17E-04	135.18	342.50	232.1	588.0
100152403921W400	15-24-2	1635.35	1.64	2.64E-04	206.42	441.37	354.4	757.8
100152903401W500	15-29-1	2633.15	1.12	3.11E-04	49.03	160.12	84.2	274.9
100162603924W400	16-26-1	1854.00	3.90	8.39E-05	160.12	342.49	274.9	588.0
100162603924W400	16-26-2	1853.20	3.47	1.21E-03	53.30	206.34	91.5	354.3
100162603924W400	16-26-3	1850.05	3.37	1.34E-02	16.26	32.05	27.9	55.0
100163604123W400	16-36-1	1726.20	1.76	1.60E-04	147.13	733.00	252.6	1258.5
100163604123W400	16-36-2	1723.50	1.03	5.59E-05	135.38	568.99	232.4	976.9
102082705127W400	08-27-1	1632.20	2.66	1.40E-04	174.40	568.84	299.4	976.6

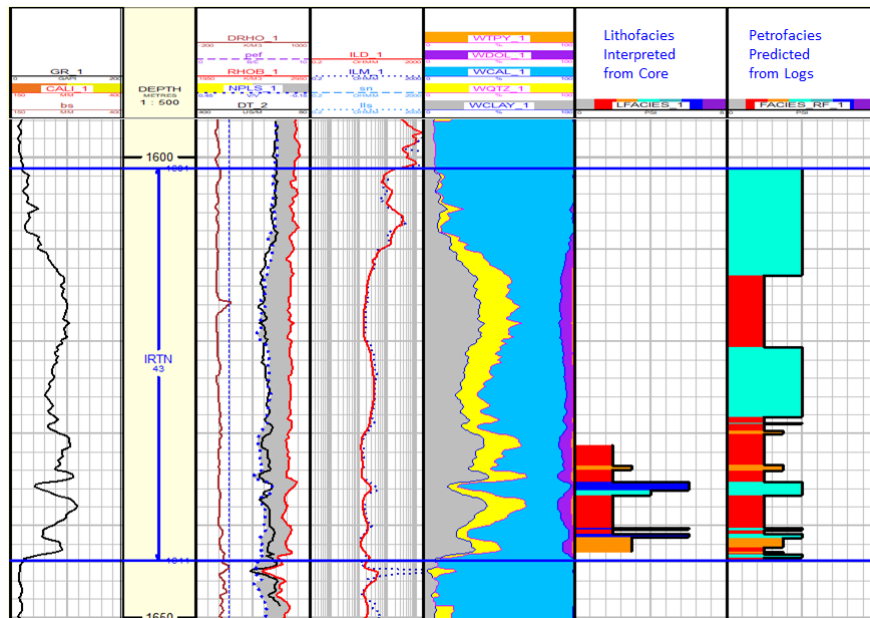


Figure 5. Log-predicted facies compared to lithofacies interpreted from core, well 15-24-39-21W4.

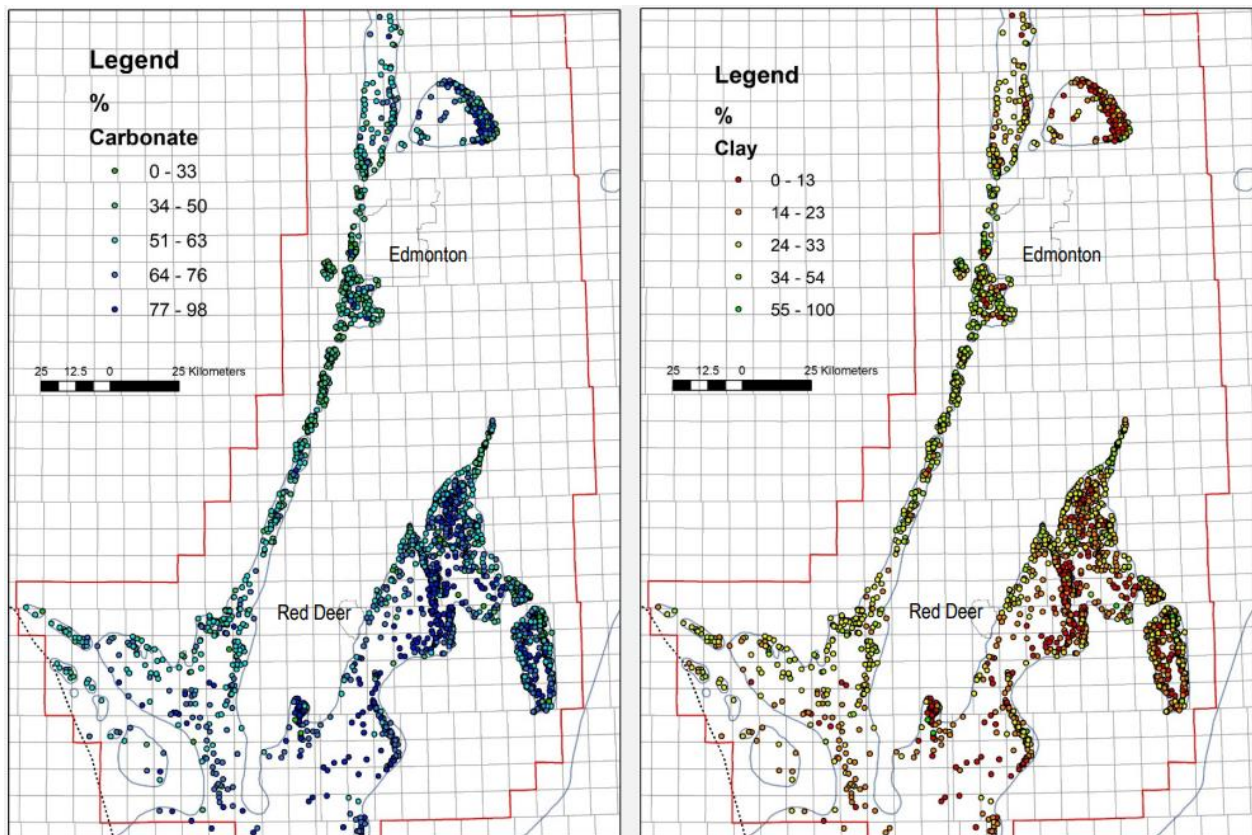


Figure 6. Ireton regional mineralogy distribution predicted from logs.

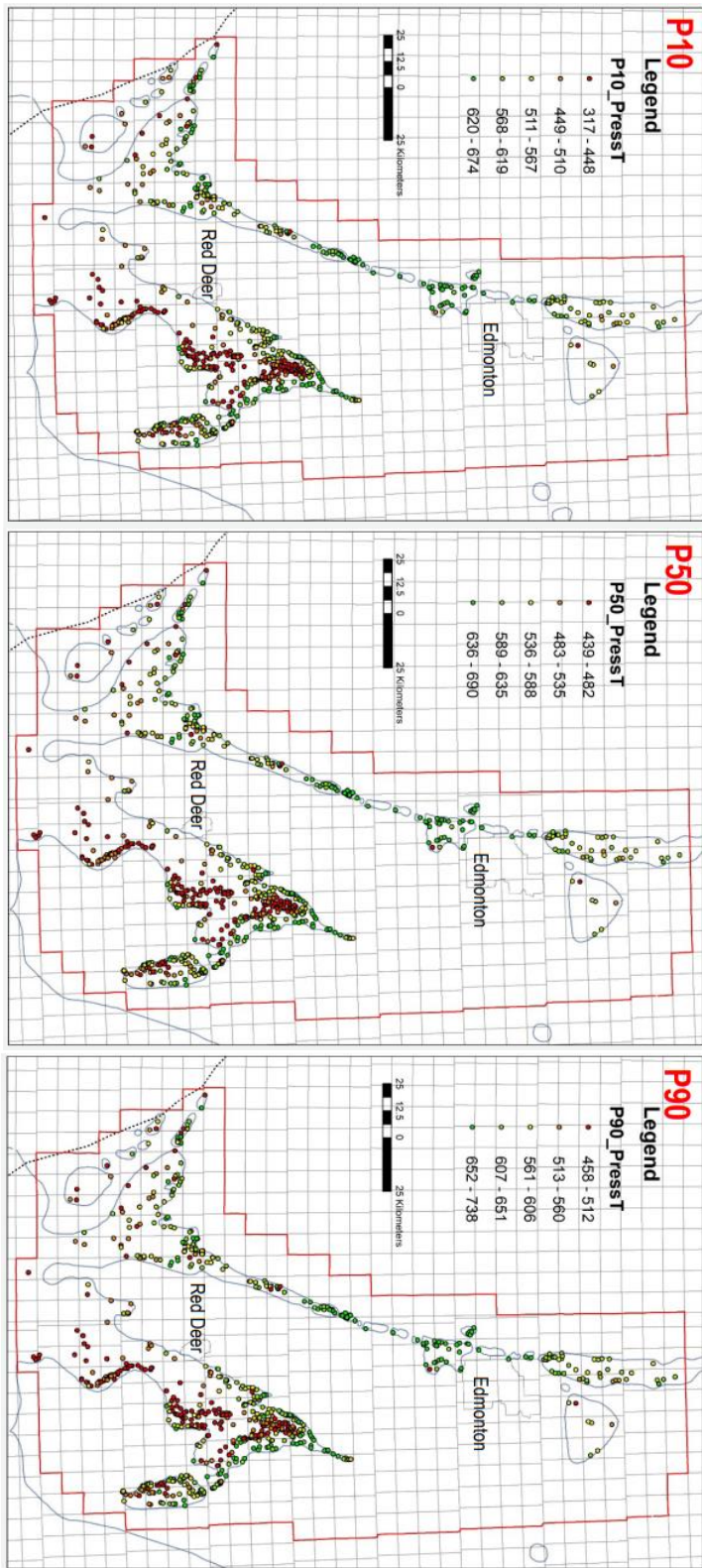


Figure 7. Regional Distribution of Threshold Pressure (psi) from Monte Carlo Simulation